HHS Public Access

Author manuscript

Exp Mech. Author manuscript; available in PMC 2022 January 01.

Published in final edited form as:

Exp Mech. 2021 January ; 61(1): 191–201. doi:10.1007/s11340-020-00664-8.

Left ventricular geometry, tissue composition, and residual stress in High Fat Diet Dahl-Salt sensitive rats

M. R. Grobbel[1], **L. C. Lee**[1], **S. W. Watts**[2], **G. D. Fink**[2], **S. Roccabianca**[1]

[1]Michigan State University, Mechanical Engineering Department

[2]Michigan State University, Pharmacology & Toxicology Department

Abstract

Background: Hypertension drives myocardial remodeling, leading to changes in structure, composition and mechanical behavior, including residual stress, which are linked to heart disease progression in a gender-specific manner. Emerging therapies are also targeting constituent-specific pathological features. All previous studies, however, have characterized remodeling in the intact tissue, rather than isolated tissue constituents, and did not include sex as a biological variable.

Objective: In this study we first identified the contribution of collagen fiber network and myocytes to the myocardial residual stress/strain in Dahl-Salt sensitive rats fed with high fat diet. Then, we quantified the effect of hypertension on the remodeling of the left ventricle (LV), as well as the existence of sex-specific remodeling features.

Methods: We performed mechanical tests (opening angle, ring-test) and histological analysis on isolated constituents and intact tissue of the LV. Based on the measurements from the tests, we performed a stress analysis to evaluate the residual stress distribution. Statistical analysis was performed to identify the effects of constituent isolation, elevated blood pressure, and sex of the animal on the output of both experimental measures and modeling results.

Results: Hypertension leads to reduced residual stress/strain intact tissue, isolated collagen fibers, and isolated myocytes in male and female rats. Collagen remains the largest contributor to myocardial residual stress in both normotensive and hypertensive animals. We identified sex-differences in both hypertensive and normotensive animals.

Conclusions: We observed both constituent- and sex-specific remodeling features in the LV of an animal model of hypertension.

Corresponding Author: S. Roccabianca; roccabis@egr.msu.edu; Phone: 517-432-3185; Fax: 517-353-1750.

CONFLICT OF INTEREST: The authors declare that they have no conflict of interest.

INTRODUCTION

Cardiovascular disease, specifically hypertension, has been shown to alter the left ventricle (LV) tissue structure, composition, and ultimately mechanical behavior [1,2]. Exposed to high afterload over a prolonged period of time, pathological features such as myocyte hypertrophy, fibrosis, and elevated resting tension of the myocytes are developed in the LV, which in turn produce concentric hypertrophy globally [3,4]. These microstructural pathological changes can also affect the residual stress/strain distribution in the LV as shown in previous studies, which reported a larger opening angle (OA) in the intact hearts subjected to pressure overload by aortic banding [5] but a lower opening angle in the intact embryonic chick heart also subjected to pressure overload [6]. Characterization of residual stress/strain is important as these quantities may affect the transmural sarcomere length distribution [7] that may in turn affect myocyte force generation [8]. Studies on changes of the residual stress/strain associated with pressure overload have, however, focused on the bulk tissue mechanical response and do not distinguish the contributions of the tissue constituents. Understanding the contribution of the constituents is important because novel therapies have been proposed to target key pathological features, such as attenuating myocardial fibrosis [9] and reducing myocyte titin stiffness [10]. Moreover, most studies were also performed without considering sex as a biological variable that may be important in hypertension. This is especially so given that there are observed sex-differences in this disease, such as its prevalence and mechanisms [11]. To address this issue, our group has shown in a recent study that the isolated collagen fibers and isolated myocytes from the healthy LV have significantly different residual stress/strain distributions between each other and when compared to the intact tissue [12]. Here, we report how a pathological increase in blood pressure affects the residual stress/strain distribution of the isolated collagen fibers and isolated myocytes in the LV. The objectives of this study are (1) to isolate the contribution of the collagen fiber network and the myocytes to the residual stress/strain distribution in the LV wall of hypertensive Dahl-Salt sensitive rats fed with high fat diet; (2) to quantify the effect of hypertension on the LV remodeling by comparing the myocardial characteristics, specifically geometry and tissue composition, of hypertensive animals to those of normotensive animals; and (3) to identify possible sex-specific features in the residual stress/strain distributions within the LV wall, both in normotensive and hypertensive conditions.

METHODS

Tissue preparation –

Dahl-Salt sensitive (Dahl-SS) rats, both male (M) and female (F), were fed with control fat diet (CD, 10 kcal% from fat, n = 15 M, n = 15 F) and high fat diet (HFD, 60 kcal% from fat, n = 15 M, n = 15 F) for 24 weeks starting at 3 weeks of age [13,14]. All animal protocols used in this study were approved by MSU Institutional Animal Care and Use Committee. In the terminal study, the whole heart was isolated and we obtained two ring-shaped samples that exposed the LV and the right ventricle (RV) by performing three lateral cuts. Of the two samples obtained from each heart, we fixed one for histological analysis and used the other for tissue constituents' isolation and then an OA test. The samples were divided equally into 3 groups: intact tissue, isolated collagen fibers, and isolated myocytes. To isolate the

constituents, we followed previously published protocols [12]. To prevent active muscle contraction while testing, both the isolated myocytes and intact tissue groups were soaked in a Krebs buffer containing 2,3-butanediome monoxime (BDM, myosin inhibitor) for 45 minutes prior and for the duration of the OA experiments [13]. After treatment and before the OA test, we obtained pictures of each sample to measure the outer diameter and thickness.

Opening angle test –

Following the procedure described in [12], a radial cut was first applied through the LV's wall (opposite to the RV). Thereafter, pictures of the sample were taken for a period of 90 minutes. The OA was quantified by analyzing the images (using ImageJ) following a graphic procedure reported in [12].

Histology –

Tissue samples were fixed in formalin (10% solution) for 72 hours and stored in a 30% ethanol solution until they were embedded in paraffin wax. The samples were then sectioned and stained with Picrosirius red (PSR) staining to highlight collagen fibers. After imaging (performed with a Nikon Eclipse 80i microscope with 10 × magnification; n = 2 for each group), we evaluated the collagen area fraction (CAF) using a custom Matlab code.

Mechanical testing and constitutive model –

An additional set of LVs of male and female Dahl-SS rats (fed either with HFD or CD) as well as male and female Sprague Dawley rats were mechanically tested. First, we obtained two ring-shaped samples from each heart; second, we divided the samples into two groups: isolated collagen and isolated myocytes (isolation protocols are specified in the *Tissue preparation* section). Third, the samples were mounted on a uniaxial tensile tester using two loops of suture (the bottom suture tied to a rigid clamp and the top suture attached to a 250g capacity load cell, LSB200, Futek), submerged in a bath with a Krebs buffer containing 2,3-BDM [13], and subjected to the following mechanical test protocol: 5% stretch for 10 cycles (preconditioning), 10% stretch for 5 cycles, 20% stretch for 5 cycles, and 30% stretch for 5 cycles. All loading was applied at a speed of 0.15 mm/s; the movement and all measurements (from the load cell and a 1.6MP Android camera mounted in front of the sample) were all controlled simultaneously through LabView. After testing, we evaluated the Cauchy stress and stretch from the axial force (load cell output) and the elongation data (Android camera output) recorded during the last loading curve of the protocol. Figure 1 shows the experimental values of Cauchy stress – stretch for a set of representative samples (symbols in the Figure represent collected data). The sample was considered incompressible, and the geometrical characteristics were evaluated from pictures of the side- and front-view of the sample before each set of loading cycles.

We then used an isotropic, exponential strain energy function [15,16] to describe the mechanical behavior of each isolated constituent, namely $W_c(\boldsymbol{C})$ for isolated collagen and $W_m(\boldsymbol{C})$ for isolated myocytes, given as

$$W_c(\boldsymbol{C}) = c_c\left(e^{k_c(\mathrm{tr}(\boldsymbol{C})-3)}-1\right),\quad W_m(\boldsymbol{C}) = c_m\left(e^{k_m(\mathrm{tr}(\boldsymbol{C})-3)}-1\right), \tag{1}$$

where c_c and c_m are material parameters with the dimension of a stress, and k_c and k_m are dimensionless material parameters; $\boldsymbol{C}$ is the right Cauchy-Green tensor, defined as $\boldsymbol{C} = \boldsymbol{F}^{\mathrm{T}}\boldsymbol{F}$, and $\boldsymbol{F} = diag\left[\lambda, \frac{1}{\sqrt{\lambda}}, \frac{1}{\sqrt{\lambda}}\right]$ is the deformation gradient tensor associated with the uniaxial tensile test with λ being the stretch in the direction of loading (i.e., circumferential direction). Material parameters were estimated by using the *lsqnonlin* function of Matlab to minimize the normalized root mean square deviation (NRMSD) between the experimental ($\boldsymbol{t}_{exp}$) and theoretical ($\boldsymbol{t}_{th}$) values of the Cauchy stress for each value of the applied stretch [17], defined as

$$NRMSD = \frac{1}{t_{exp}^{max}}\sqrt{\frac{\sum_{i=1}^{N}\left(t_{th}^{i}-t_{exp}^{i}\right)^2}{N}}. \tag{2}$$

where N is the number of experimental datapoints collected and t_{exp}^{max} is the maximum value of Cauchy stress reached for each sample during the mechanical test. We obtained eight sets of parameters (one for isolated collagen and one for isolated myocytes) for both male and female, for Sprague Dawley and for Dahl-SS animals. Values of the material parameters for each group are shown (as mean +/− stdev) in Table 1. The mean values of material parameters for each group are then employed in the residual stress analysis. Due to the low statistical power of this portion of the study, we will not comment on differences in material parameters between the groups. In addition, the limited availability of Dahl-SS animals on each diet, allowed us to test mechanically only a low number of animals on CD (2 males and 2 females) and HFD (2 males and 2 females). For this reason, we employed the average of material parameters between diets for each male and female animal in the current study. This is a limitation of the study. To limit the impact of this limitation on the meaningfulness of this analysis we will report results for both stress and stretch residual stress fields (see Results section).

Finally, the strain energy function of the intact tissue was described by the weighted averaged of the constituents as

$$W_{intact}(\boldsymbol{C}) = \phi_c W_c(\boldsymbol{C}) + \phi_m W_m(\boldsymbol{C}) \tag{3}$$

where Φ_c and Φ_m represent the area fractions of the collagen (CAF) and myocytes ($\Phi_m = 1 - \Phi_c$) evaluated in the intact tissue (see *Histology* section). Note that from Equation (3), one can recover the isolated collagen fibers strain energy function when $\Phi_c = 1$ and $\Phi_m = 0$ and the isolated myocytes strain energy function when $\Phi_c = 0$ and $\Phi_m = 1$.

Residual stress modeling –

We used the continuum mechanics theory of large deformation to model the residual stresses in the LV [12,18–20]. For each sample, we have evaluated the Cauchy stress across the wall as

$$\boldsymbol{t}_\alpha = -p_\alpha \boldsymbol{I} + 2\boldsymbol{F}\frac{\partial W_\alpha(\boldsymbol{C})}{\partial \boldsymbol{C}}\boldsymbol{F}, \tag{4}$$

where W_α is the appropriate strain energy function (with $\alpha = c, m, intact$ respectively; see Equations (1) and (3)), p_α is a Lagrange multiplier used to enforce incompressibility, and $\boldsymbol{F}$ and $\boldsymbol{C}$ are the deformation gradient and the right Cauchy-Green deformation tensor representing the mapping from the stress-free, cut configuration (coordinates R, Θ, Z) to the load-free, closed configuration (coordinates ρ, θ, z). Specifically, for each sample, $\boldsymbol{F}$ is written as

$$\boldsymbol{F} = \begin{bmatrix} \frac{\partial \rho}{\partial R} & 0 & 0 \\ 0 & \frac{\rho}{R}\frac{2\pi}{2\pi - \Phi} & 0 \\ 0 & 0 & \Lambda_z \end{bmatrix}, \tag{5}$$

where Φ represents the opening angle for each sample. Finally, the Cauchy stress described by Equation (4) must satisfy the radial and axial equilibrium equations in the load-free, closed configuration. See the Appendix section for details about the stress evaluation procedure. Finally, in order to draw comparisons between groups, we have identified a subset of characteristic points on the transmural distribution of stress across the wall, which can be seen in Figure 2.

RESULTS

As previously reported [14,21], Dahl-SS rats fed with HFD for 24 weeks have a significantly higher body weight and mean arterial pressure (MAP) as measured by the tail-cuff plethysmography method (MAP, 155 ± 4.7 mmHg for M; 162 ± 5.7 mmHg for F) when compared to their counterparts that were fed with a CD (MAP of 124 ± 5.6 mmHg for M; 142 ± 8.1 for F) for both sexes. It is important to note that, while the CD animals have significantly lower MAP compared to HFD, their arterial pressure is still considered to be above the hypertension threshold (MAP ~ 106 mmHg [22]). For this reason, we will also compare our results to those collected previously from normotensive (NT) Sprague Dawley rats [12] (MAP: 105 ± 3.3 mmHg [23]). While we are aware that to compare different animal strains is not ideal, we believe that it is important to establish a baseline for NT animals, as reported in previous studies [24,25].

Figure 3 shows the geometric characteristics indexed by the LV cross-sectional area for the animal groups considered. Overall, LVs in the HFD group have a larger cross-sectional area compared to the CD for both sexes and all tissue treatments (difference not significant for isolated myocytes and isolated collagen fibers in M, and for intact tissue in F). The female LVs are also smaller than their male counterpart (difference not significant for isolated myocytes and isolated collagen fibers for HFD and for isolated collagen fibers in CD). When compared to NT animals, both HFD and CD animals have larger cross-sectional areas.

Figure 4 (a–f) shows images of histological slides stained with PSR for representative samples. Figure 4 (g) shows the values of collagen area fraction (CAF) for each group; we observe no difference in CAF when comparing CD to HFD and male to female. When comparing the hypertensive animals (CD + HFD) to NT animals, we also observe no significant difference in CAF. Male CD samples, however, have a higher CAF when compared to NT males, whereas female HFD samples have a lower CAF compared to those from the corresponding NT group. Finally, female NT samples have a higher CAF when compared to those from their male counterpart.

We report the OA results collected for all groups at the 90 min mark, motivated by the results reported in [12]. As shown in Figure 5 (a), the OA for isolated collagen fibers is highest, followed by that of the intact tissue, and that of the isolated myocytes for both sexes and both diets (difference not significant for intact tissue vs isolated collagen in CD F), similar to that reported in NT animals [12]. Comparison of the OA between CD and HFD groups in Figure 5 (b) reveals that the OA is similar for intact tissues in both sexes, but HFD males have a lower OA compared to CD males in isolated myocytes (value is unchanged in females) and HFD females have a higher OA when compared to CD females in isolated collagen fibers (value is unchanged in males). Comparing these results to that of the NT animals reveals that increased MAP could lead to a decrease in the OA in the intact tissue, isolated collagen fibers, and isolated myocytes.

Consistently with what is observed for the OA's values, the stress and stretch analyses show overall higher residual stresses/stretches in the isolated collagen fibers and lower stresses/stretches in the isolated myocytes when compared to intact tissue for all quantities' components (see Figure 2 for definition) considered and for all groups. However, these differences are more prominent in female than they are in male when considering both residual stress or stretch distributions. When looking at stresses specifically, while differences are all significant for all female groups (i.e., when comparing isolated constituents to one another and when comparing isolated constituents to intact tissue), in male hypertensive animals, differences are mostly not significant when comparing intact tissue to isolated collagen fibers and isolated myocytes, for both CD and HFD. For the male hypertensive animals, however, all the residual stress components calculated for isolated collagen fibers remain significantly higher than that for isolated myocytes. A similar trend can be observed in the residual stretch distributions as well, with two exceptions: (1) in CD female animals we observe no differences between intact tissue and isolated collagen fibers (true for all stretch markers considered) and (2) in HFD male animals, we do observe a significant difference between intact tissue and collagen fibers (true for most stretch markers considered and specified in Figure B1 in Appendix B). As a representative subset of stress components, we show the maximum circumferential tensile stress and stretch in Figure 6 (a) and (b) respectively – focusing on highlighting differences between constituents.

When analyzing the effect of high blood pressure on the residual stress and stretch distributions, we observe that, overall, NT animals have higher residual stresses/stretch when compared to hypertensive animals (both CD and HFD) for both male and female. The differences between NT and both cases of hypertensive were consistently significant for all samples collected from the female animals, while it was only significant in the males'

isolated collagen fibers and slightly (P = 0.07) for the CD isolated myocytes (insignificant for the HFD isolated myocytes). Moreover, we have found no differences when comparing the stress/stretch levels between CD and HFD animals, in both male and female, the only exception being potentially an increase in collagen residual stresses/stretches when comparing CD to HFD (not significant). Figure 7 (a) and (b) shows the maximum value of circumferential stress and stretch, as a representative subset, focusing on highlighting the comparison between NT and hypertensive animals, and between male and female animals, for isolated myocytes (left), intact tissue (center), and isolated collagen fibers (right).

From Figure 7 we can also infer the effect of sex on the stress distribution. In NT animals, females have significantly higher values for all the residual stress/stretch components when compared to males. In hypertensive animals, the stress in the female hearts remains significantly higher than that in the male for the isolated collagen fiber network, results specific to the residual stress distribution (the residual stretches show no sex-difference in the isolated collagen fibers). In addition, the difference in residual stress/stretch characteristics between male and female animals is lost for both intact tissue and isolated myocytes (or the relation is reversed, like in isolated myocytes in CD Dahl SS rats, where males have a higher stress than females).

Finally, Figure 8 shows the relative location across the LV wall (measured through the dimensionless radius) of the circumferential neutral axis (location along the radius where the circumferential stress is null) for intact tissue in both male and female animals. The neutral axis in female LV moves significantly closer to the luminal layer with the increase in blood pressure, while it remains unchanged for male hearts.

DISCUSSION

We have measured the changes in the OA and residual stresses/stretch, associated with hypertension, of the intact cardiac tissue and tissues with isolated constituents in both male and female rats. The key findings of this study are 1) OA in the intact tissue, isolated collagen fibers, and isolated myocytes are all reduced with hypertension in male and female rats; 2) All residual stress/stretch components are highest in the isolated collagen fibers, followed by the intact tissue and isolated myocytes in both male and female rats; 3) All the residual stress/stretch components are also reduced with hypertension in both male and female rats; and 4) All the residual stress/stretch components in the female NT rats are significantly higher than those in the male NT rats, but the difference is lost with hypertension in the intact tissue and tissue with isolated myocytes.

Our finding of a reduction in OA with hypertension is consistent with a previous study on the embryonic chick heart [6], where they found the OA was decreased from 31 ± 10 to −8 ± 12 degrees 12 hours after induction of pressure overload. This finding is, however, in contrast to a previous study, which reported that the OA of the intact tissue is increased with pressure overload [5]. This discrepancy may be due to 1) the different approach used to generate pressure overload – aortic banding [5] vs. Dahl-SS animals that are genetically predisposed to high blood pressure [24] used here and 2) the different stages of remodeling – 3 weeks after banding [5] *vs.* 24 weeks of CD or HFD here. Consequently, the tissues

studied here may correspond more to the decompensated phase of remodeling *vs.* compensated in [5]. Finally, the OA reported in [5] is higher in hypertensive animals compared to controls one week after banding (i.e., after onset of pressure overload); however, the authors reported no statistically significant difference between the groups 3 weeks after surgery. This could support an inversion between the values of the OA of treated *vs.* control animals in later time points, leading to a lower value of OA in hypertensive animals long-term.

Our analysis went further to estimate the OA angle (residual strains) of the isolated collagen fibers and myocytes as well as their corresponding residual stresses, which previous studies are lacking [26]. We found that residual stresses associated with the isolated collagen fibers are significantly higher than that of the isolated myocytes and the intact cardiac tissue. This suggests that collagen fibers remain the stronger contributor to the residual stress distribution in remodeled hypertensive LVs. The residual stresses of the constituents (especially that of the isolated collagen fibers) as well as the intact tissue are all reduced with hypertension. Based on a previous study [27], a reduction in the residual stress may contribute to the increased LV stiffness that is typically associated with hypertension [28]. Moreover, males fed with HFD have decreased OA and residual stresses/stretches in isolated myocytes when compared to males fed with CD, and females fed with HFD have increased OA and residual stresses/stretches in isolated collagen fibers when compared to females fed CD. These results may suggest a potential increase in the contribution of the collagen fibers and a decrease in the contribution of the myocytes to the residual stress distribution as MAP increases, despite having no changes in the overall CAF between NT and hypertensive animals (Figure 4). We have also observed, only in female animals, that the circumferential neutral axis moves closer to the inner radius with an increase in MAP (Figure 8), suggesting a larger portion of the wall is in tension due to residual stresses. This could be associated with the observed changes in circumferential systolic strain distribution across the myocardial wall in hypertension [29].

We have also investigated sex differences in residual stresses/stretches in this study, and have found that residual stresses/stretches in the female rats are significantly higher than those in the male rats under normotensive condition. This difference, however, is lost or inverted with hypertension in the intact tissue as well as the tissue with isolated myocytes, suggesting that hypertension has a bigger effect on the residual stress field in female rats than male rats. In fact, residual stresses in the female LV decrease with hypertension on average 77% for intact tissue and 46% for isolated myocytes, while in the male LV, on average, residual stresses in intact tissue decrease by 48% and in isolated myocytes increase by 37% (% change evaluated for the maximum circumferential stress, Figure 7 (a)). This suggests that the remodeling process in the LV could have sex-specific traits, a hypothesis supported also by observation in a previous publication. First, gender-differences in heart failure preserved ejection fraction (HFpEF), of which hypertension is a major risk factor, have long been observed [30,31]. Besides affecting more women, it is also found in a study that LV diastolic function is more impaired with a greater diastolic stiffness present in women than men in HFpEF [32]. Our finding that a larger reduction in residual stresses/stretches associated with hypertension (that in turn may cause an increase in LV stiffness based on a previous study

[27]) is consistent with this clinical observation, despite the decrease in CAF in the hypertensive samples compared to NT samples in females.

Finally, we have also analyzed changes in the overall geometry of the LV, and we observed an increase in the LV cross-sectional area following a pathological increase in MAP, which confirms what was previously reported [5]. These differences seem to be associated with an increase in both LV thickness and diameter. Specifically, both outer diameter and thickness increase with an increase in MAP in female rats. In male rats, both outer diameter and thickness are higher in the hypertensive animals for the isolated constituents, while the thickness increases moderately in the intact tissue.

This study has some limitations. First, the duration of the opening angle experiment was longer than what was previously published by other groups [33]. The duration of the overall experiment was determined based on a terminating criterion that the rate of change in angle is equal or less than ~0.2°/min on average for all the experimental groups. This is because we seek to determine the opening angle at a steady state that corresponds to the true residual stress found in the left ventricle in its passive state. Indeed, the duration is longer than those found in previous studies (e.g., [33] that measured the opening angle within 30 seconds of radial cutting to determine the residual strain without ischemic contracture). While it is possible that the measurement performed on intact tissue and isolated myocytes is affected by muscle contraction, we performed all measurement in a solution containing a myosin inhibitor (BDM) to limit this effect. Furthermore, we collected datapoints throughout the 90 minutes of the experiment, including at the time of the cut (within 30 sec); and the statistical analysis for the measurements collected at the time of the cut seems to confirm the relations established considering the OA measured at 90 min (data not shown). Second, we are using material parameters collected from a uniaxial tensile test and employing an isotropic model to describe the LV constituents in the stress analysis. While we know that the myocardium does not behave as an isotropic material, we were constrained by the experimental capabilities in our facilities. To decrease the effect of this limitation on the analysis, we have decided to, first, include results for both the residual stress and stretch distributions, and second, to focus our analysis on the circumferential distribution of stress, which is the direction better characterized by both the experimental set up and the choice of strain energy function. A more precise characterization of the tissue, which includes biaxial information and more accurate description of the fiber distributions across the wall, will be the focus of future studies.

CONCLUSION

In this study, we reported the changes in the LV geometry, composition, and residual stress distribution in Dahl-SS rats of both sexes fed with CD or HFD. In summary, we show that 1) animals fed with HFD have a larger LV cross-sectional area compared to CD in both sexes; 2) CAF is not affected by diet; 3) OA and residual stresses/stretches of collagen fibers is largest followed by that of the intact tissue and then isolated myocytes in hypertension; 4) OA of isolated collagen fibers from the LV of male rats fed with HFD is lower than those fed with CD, whereas the OA of isolated myocytes from the LV of female rats fed with HFD is higher those fed with CD; 5) OA and residual stresses/stretches of the LV in the

hypertensive animals are lower than that of the NT animals; and 6) the residual stresses/stretches in the female NT rats are higher when compared to the male NT rats, while we observe no difference between female and male hypertensive rats in the intact tissue and tissue with isolated myocytes.

ACKNOWLEDGMENT:

This work was supported by NSF CMMI GRANT #1933768. We kindly acknowledge Kibrom M. Alula, Emma Darios Flood, and Ari Hollander for their help with animals and experiments.

APPENDIX A

In order to calculate the stress distribution across the wall given by Equation (4), we used each sample's individual geometry from the open configuration (R_i, R_o, Φ), along with their pooled material properties (c_c, k_c, c_m, k_m) and constituent area fractions (Φ_c, Φ_m). It should be noted that when using Equation (3) for intact tissue, Φ_c and Φ_m were equal to their experimental values. For each sample, the inner and outer radii and axial stretch of the closed, load-free configuration (ρ_i, ρ_o, Λ_z) were estimated by using the deformation gradient in Equation (5) and allowing the closed configuration to reach radial and axial equilibrium (using the *lsqnonlin* function on Matlab)—i.e.,

$$\int_{\rho_i}^{\rho_o} \frac{1}{\rho}\left(t_{\theta\theta} - t_{\rho\rho}\right) d\rho = 0,$$

$$\int_{\rho_i}^{\rho_o} \rho\left[2t_{zz} - \left(t_{\theta\theta} + t_{\rho\rho}\right)\right] d\rho = 0.$$

Additionally, an assumption of incompressibility was made for Equation (5), resulting in a third equation used to solve for the unknown geometry:

$$\rho_o = \sqrt{\rho_i^2 + \frac{1}{\Lambda_z}\frac{2\pi}{2\pi - \Phi}\left(R_o^2 - R_i^2\right)}$$

Finally, for each sample, we had individual geometry measurements (R_i, R_o, Φ, ρ_i, ρ_o, Λ_z), pooled material properties from their breed and sex (c_c, k_c, c_m, k_m) and collagen and myocytes area fractions (Φ_c, Φ_m) for the intact tissue, measured for each breed, sex, and diet (i.e. HFD or CD). Using all of this information, we were able to calculate the radial, circumferential, and axial stresses for each group as functions of their non-dimensional radii.

APPENDIX B

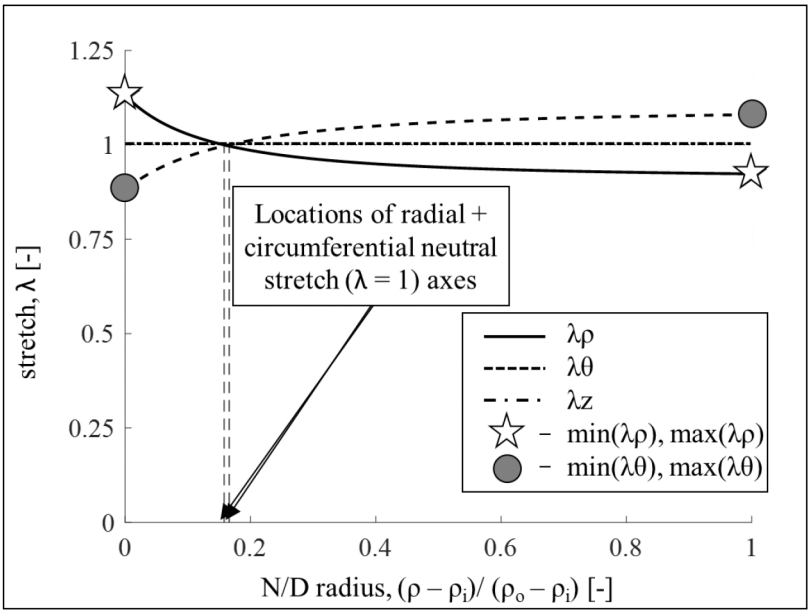

Figure B1.

Transmural residual stretch distribution for one representative sample. Radial stretch (solid line), circumferential stretch (dashed line), and axial stretch (dashed dotted line). For each sample, after evaluating the principal stretches distribution, as shown, we identified values of interest to compare across groups. Specifically, we calculated the minimum and maximum values of the radial and circumferential stretches. Note: while the axial stretch assumes in most cases values close to 1, no plain strain assumption was made.

REFERENCES

1. Rossi MA, 1998. Pathologic fibrosis and connective tissue matrix in left ventricular hypertrophy due to chronic arterial hypertension in humans. Journal of hypertension, 16(7), pp.1031–1041. [PubMed: 9794745]
2. Omens JH, Milkes DE and Covell JW, 1995. Effects of pressure overload on the passive mechanics of the rat left ventricle. Annals of biomedical engineering, 23(2), pp.152–163. [PubMed: 7605052]
3. Oktay AA and Shah SJ, 2014. Current perspectives on systemic hypertension in heart failure with preserved ejection fraction. Current cardiology reports, 16(12), p.545. [PubMed: 25326729]
4. Teo LYL, Chan LL and Lam CSP, 2016. Heart failure with preserved ejection fraction in hypertension. Current opinion in cardiology, 31(4), pp.410–416. [PubMed: 27070649]
5. Omens JH, Rodriguez EK and McCulloch AD, 1996. Transmural changes in stress-free myocyte morphology during pressure overload hypertrophy in the rat. Journal of molecular and cellular cardiology, 28(9), pp.1975–1983. [PubMed: 8899556]
6. Taber LA and Chabert S, 2002. Theoretical and experimental study of growth and remodeling in the developing heart. Biomechanics and modeling in mechanobiology, 1(1), pp.29–43. [PubMed: 14586705]
7. Rodriguez EK, Omens JH, Waldman LK and McCulloch AD, 1993. Effect of residual stress on transmural sarcomere length distributions in rat left ventricle. American Journal of Physiology-Heart and Circulatory Physiology, 264(4), pp.H1048–H1056.
8. de Tombe PP and ter Keurs HE, 2016. Cardiac muscle mechanics: sarcomere length matters. Journal of molecular and cellular cardiology, 91, pp.148–150. [PubMed: 26678623]

9. Zouein FA, de Castro Brás LE, Da Costa DV, Lindsey ML, Kurdi M and Booz GW, 2013. Heart failure with preserved ejection fraction: emerging drug strategies. Journal of cardiovascular pharmacology, 62(1), p.13. [PubMed: 23714774]
10. Krüger M, Kötter S, Grützner A, Lang P, Andresen C, Redfield MM, Butt E, Dos Remedios CG and Linke WA, 2009. Protein kinase G modulates human myocardial passive stiffness by phosphorylation of the titin springs. Circulation research, 104(1), pp.87–94. [PubMed: 19023132]
11. Ramirez LA and Sullivan JC, 2018. Sex differences in hypertension: where we have been and where we are going. American journal of hypertension, 31(12), pp.1247–1254. [PubMed: 30299518]
12. Grobbel MR, Shavik SM, Darios E, Watts SW, Lee LC and Roccabianca S, 2018. Contribution of left ventricular residual stress by myocytes and collagen: existence of inter-constituent mechanical interaction. Biomechanics and modeling in mechanobiology, 17(4), pp.985–999. [PubMed: 29478195]
13. Hajjar RJ, Ingwall JS and Gwathmey JK, 1994. Mechanism of action of 2, 3-butanedione monoxime on contracture during metabolic inhibition. American Journal of Physiology-Heart and Circulatory Physiology, 267(1), pp.H100–H108.
14. Alula KM, Biltz R, Xu H, Garver H, Laimon-Thomson EL, Fink GD and Galligan JJ, 2019. Effects of high-fat diet on sympathetic neurotransmission in mesenteric arteries from Dahl salt-sensitive rat. Autonomic Neuroscience, 222, p.102599. [PubMed: 31731103]
15. Demiray H, 1972. A note on the elasticity of soft biological tissues. Journal of biomechanics, 5(3), pp.309–311. [PubMed: 4666535]
16. Delfino A, Stergiopulos N, Moore JE Jr and Meister JJ, 1997. Residual strain effects on the stress field in a thick wall finite element model of the human carotid bifurcation. Journal of biomechanics, 30(8), pp.777–786. [PubMed: 9239562]
17. Chen S, Annaidh AN and Roccabianca S, 2020. A microstructurally inspired constitutive model for skin mechanics. Biomechanics and Modeling in Mechanobiology, 19(1), pp.275–289. [PubMed: 31396807]
18. Nevo E and Lanir Y, 1994. The effect of residual strain on the diastolic function of the left ventricle as predicted by a structural model. Journal of biomechanics, 27(12), pp.1433–1446. [PubMed: 7806551]
19. Omens JH, McCulloch AD and Criscione JC, 2003. Complex distributions of residual stress and strain in the mouse left ventricle: experimental and theoretical models. Biomechanics and modeling in mechanobiology, 1(4), pp.267–277. [PubMed: 14586695]
20. Humphrey JD and Delange SL, 2016. Introduction to Biomechanics. Springer-Verlag New York.
21. Fernandes R, Garver H, Harkema JR, Galligan JJ, Fink GD and Xu H, 2018. Sex differences in renal inflammation and injury in high-fat diet–fed Dahl salt-sensitive rats. Hypertension, 72(5), pp.e43–e52. [PubMed: 30354819]
22. Whelton PK, Carey RM, Aronow WS, Casey DE Jr, Collins KJ, Dennison Himmelfarb C, DePalma SM, Gidding S, Jamerson KA, Jones DW and MacLaughlin EJ, 2017. Guideline for the prevention, detection, evaluation, and management of high blood pressure in adults: a report of the American College of Cardiology/American Heart Association Task Force on Clinical Practice Guidelines. Journal of the American College of Cardiology, 71(6), pp.1269–1324.
23. Kandlikar SS and Fink GD, 2011. Mild DOCA-salt hypertension: sympathetic system and role of renal nerves. American Journal of Physiology-Heart and Circulatory Physiology, 300(5), pp.H1781–H1787. [PubMed: 21357502]
24. Gillis EE, Williams JM, Garrett MR, Mooney JN and Sasser JM, 2015. The Dahl salt-sensitive rat is a spontaneous model of superimposed preeclampsia. American Journal of Physiology-Regulatory, Integrative and Comparative Physiology, 309(1), pp.R62–R70.
25. Greene AS, Yu ZY, Roman RJ and Cowley AW Jr, 1990. Role of blood volume expansion in Dahl rat model of hypertension. American Journal of Physiology-Heart and Circulatory Physiology, 258(2), pp.H508–H514.
26. Omens JH, Vaplon SM, Fazeli B and McCulloch AD, 1998. Left ventricular geometric remodeling and residual stress in the rat heart. Journal of Biomechanical Engineering, 120(6): 715–719 [PubMed: 10412454]

27. Genet M, Rausch MK, Lee LC, Choy S, Zhao X, Kassab GS, Kozerke S, Guccione JM and Kuhl E, 2015. Heterogeneous growth-induced prestrain in the heart. Journal of biomechanics, 48(10), pp.2080–2089. [PubMed: 25913241]

28. Tam MC, Lee R, Cascino TM, Konerman MC and Hummel SL, 2017. Current perspectives on systemic hypertension in heart failure with preserved ejection fraction. Current hypertension reports, 19(2), p.12. [PubMed: 28233237]

29. Parikh JD, Hollingsworth KG, Wallace D, Blamire AM and MacGowan GA, 2017. Left ventricular functional, structural and energetic effects of normal aging: Comparison with hypertension. PloS one, 12(5), p.e0177404. [PubMed: 28493996]

30. Duca F, Zotter-Tufaro C, Kammerlander AA, Aschauer S, Binder C, Mascherbauer J and Bonderman D, 2018. Gender-related differences in heart failure with preserved ejection fraction. Scientific reports, 8(1), pp.1–9. [PubMed: 29311619]

31. Beale AL, Nanayakkara S, Segan L, Mariani JA, Maeder MT, van Empel V, Vizi D, Evans S, Lam CS and Kaye DM, 2019. Sex differences in heart failure with preserved ejection fraction pathophysiology: a detailed invasive hemodynamic and echocardiographic analysis. JACC: Heart Failure, 7(3), pp.239–249. [PubMed: 30819380]

32. Gori M, Lam CS, Gupta DK, Santos AB, Cheng S, Shah AM, Claggett B, Zile MR, Kraigher-Krainer E, Pieske B and Voors AA, 2014. Sex-specific cardiovascular structure and function in heart failure with preserved ejection fraction. European journal of heart failure, 16(5), pp.535–542. [PubMed: 24574260]

33. Omens JH and Fung YC, 1990. Residual strain in rat left ventricle. Circulation research, 66(1), pp.37–45. [PubMed: 2295143]

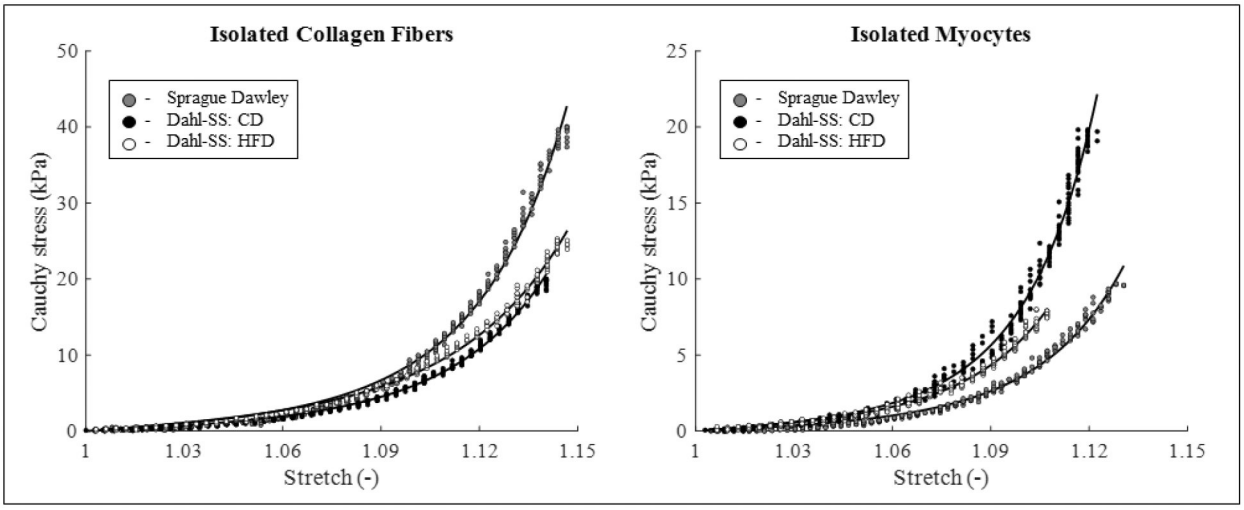

Figure 1.

Cauchy stress *vs.* stretch experimental dataset (symbols) and model best-fit description (lines) for isolated constituents, on the left collagen fibers and on the right myocytes. In each graph, a representative dataset for one male animal from each group is shown, specifically Sprague Dawley (experiments: grey circles, model: grey line), Dahl SS fed with CD (experiments: black circles, model: black line), and Dahl SS fed with HFD (experiments: open circles, model: light grey line).

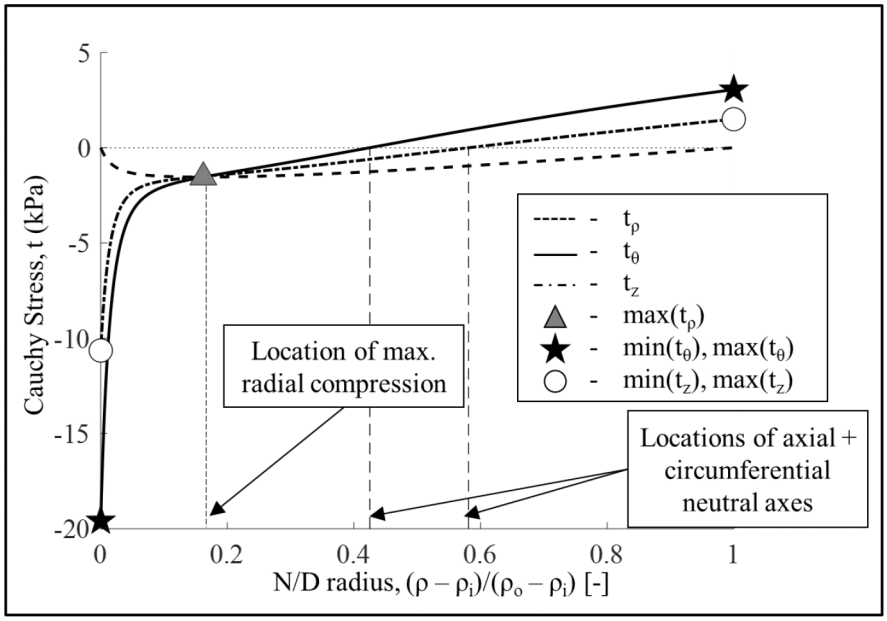

Figure 2.

Transmural residual stress distribution for one representative sample. Radial stress (dashed line), circumferential stresses (solid line), and axial stress (dashed dotted line). For each sample, after evaluating the transmural Cauchy stress distribution, as shown, we identified values of interest to compare across groups. Specifically, we calculated the minimum value of the radial stress (maximum compression) and its normalized location across the radius; the maximum (maximum tension, at the outer radius) and minimum (maximum compression, at the inner radius) values of the circumferential and axial stresses, as well as the normalized location across the wall of the circumferential and axial neutral axes.

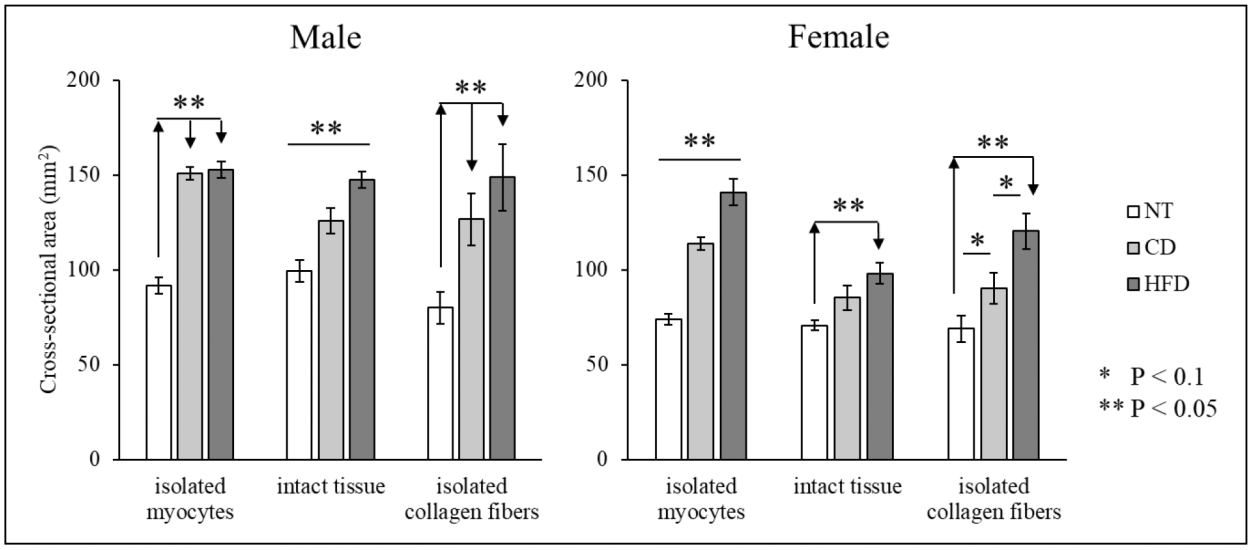

Figure 3.

Cross-sectional area evaluated for all samples (mean ± standard error). Comparison between CD and HFD for isolated myocytes, isolated collagen fibers, and intact tissue (also included data for NT).

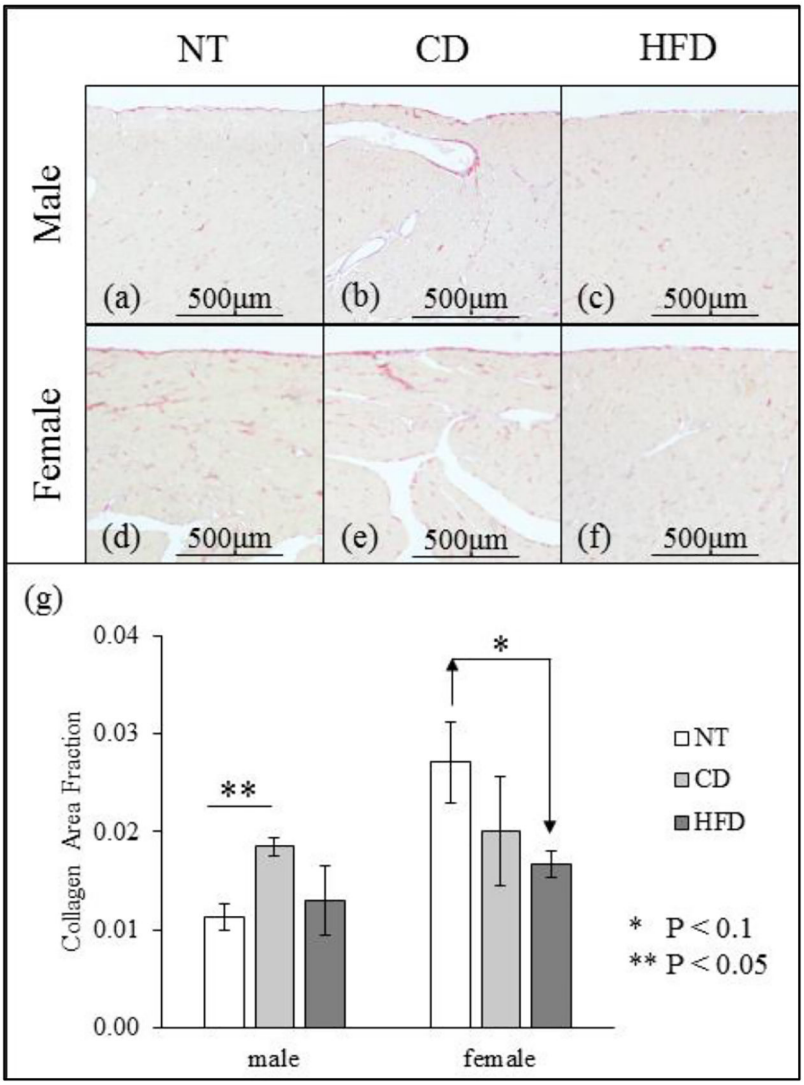

Figure 4.

(a-f) Images of picrosirius red stained slides of male (a-c) and female (d-f) LV (a, d: NT; b, e: CD; c, f: HFD). (g) Collagen area fraction evaluated for all samples (mean ± standard error).

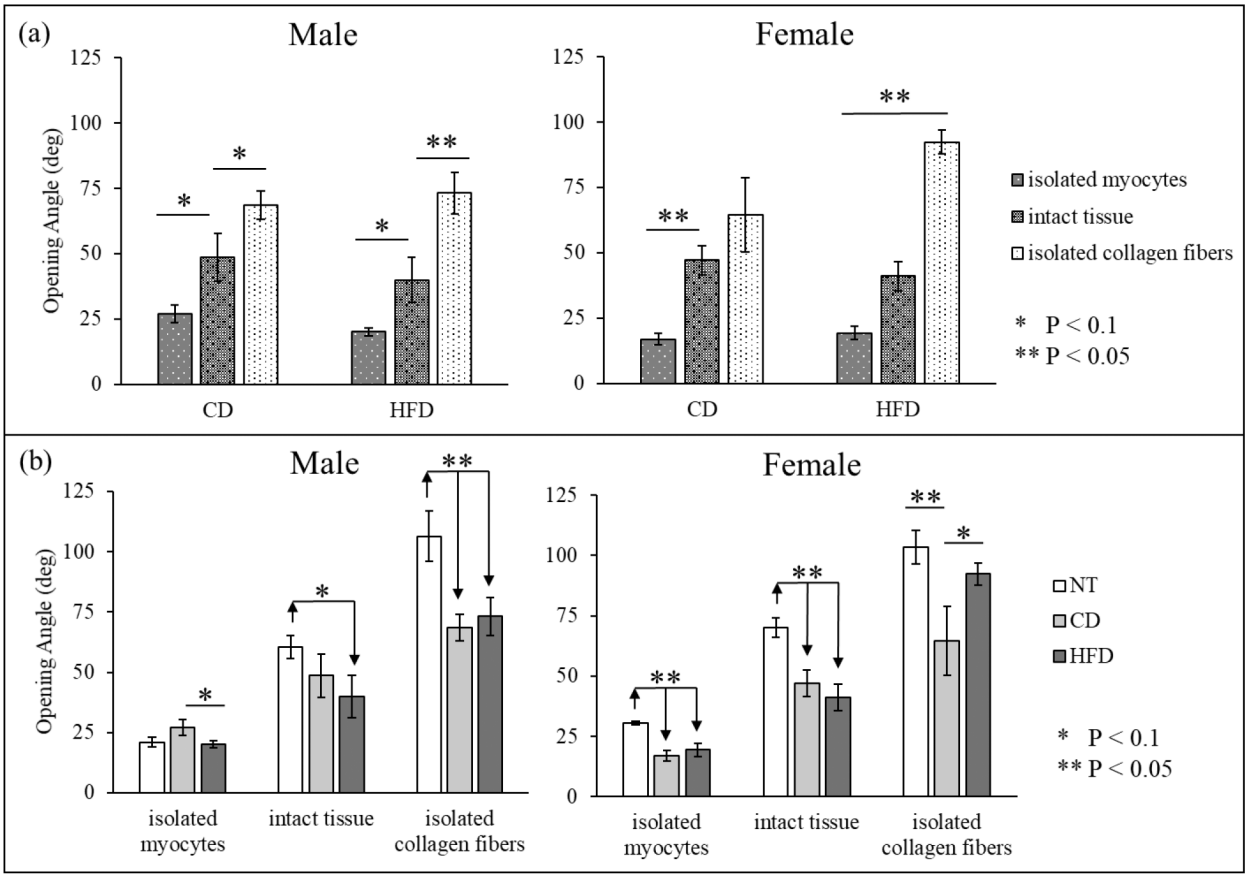

Figure 5.

Opening angle (deg) measured for all samples (mean ± standard error). (a) Comparison between isolated myocytes, isolated collagen fibers, and intact tissue for both CD and HFD. (b) Comparison between CD and HFD (also included data for NT).

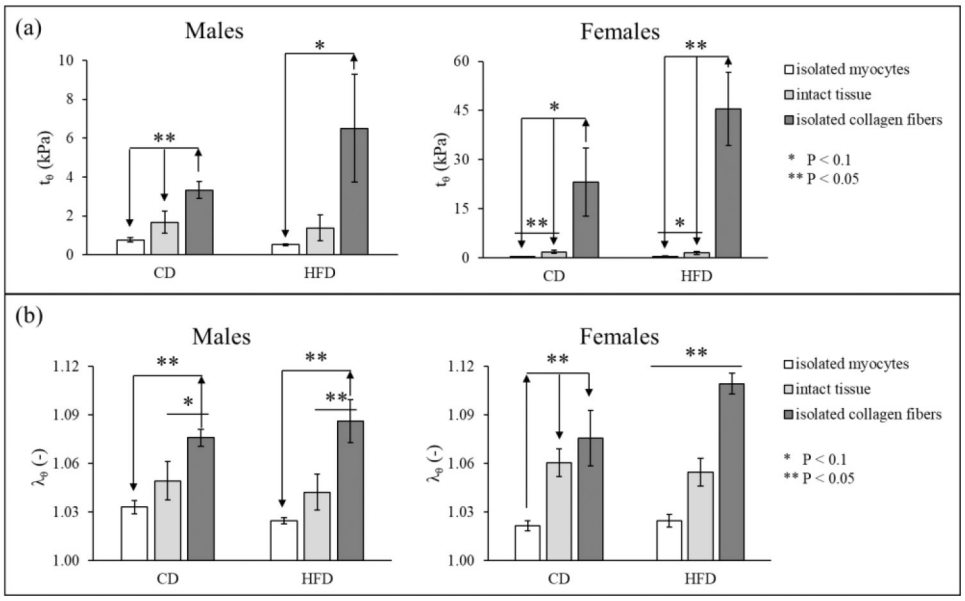

Figure 6.

Comparison between isolated myocytes, isolated collagen fibers, and intact tissue for both CD and HFD of the maximum value of (a) circumferential residual stress (t_θ, as identified in Figure 2) and (b) circumferential stretch (λ_θ) for all samples (mean ± standard error, note: the graphs have different vertical axes).

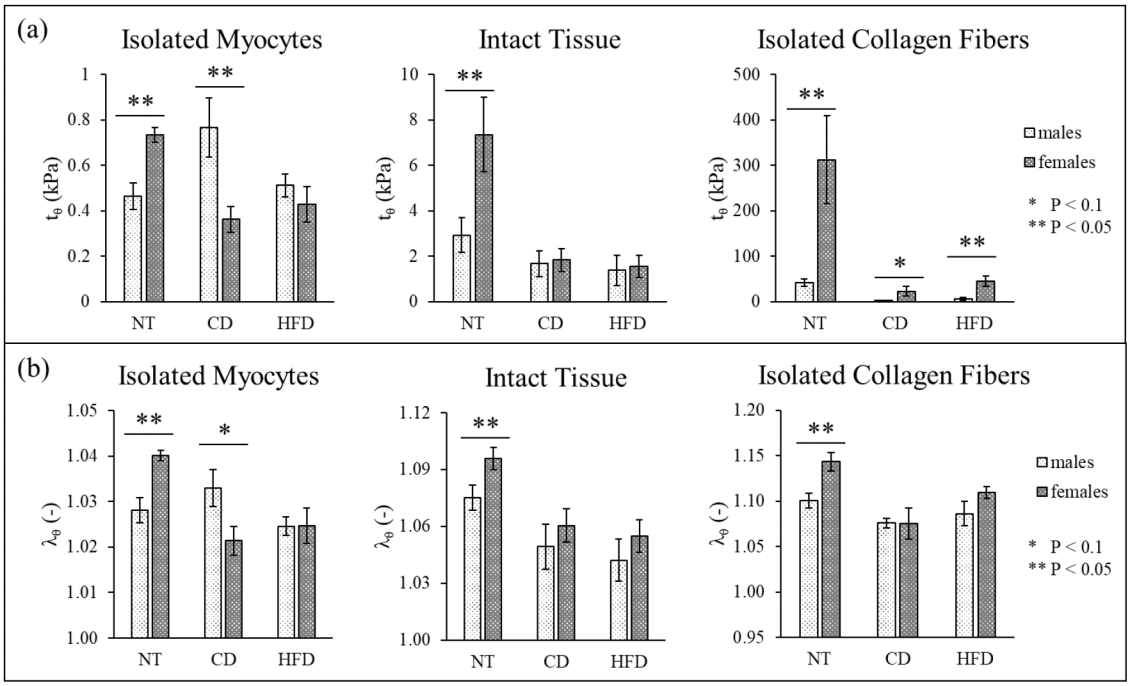

Figure 7.

Comparison between sex of the animal, including data for NT, of the maximum value of (a) circumferential residual stress (t_θ, as identified in Figure 2) and (b) circumferential stretch (λ_θ) for all samples (mean ± standard error, note: the graphs have different vertical axes).

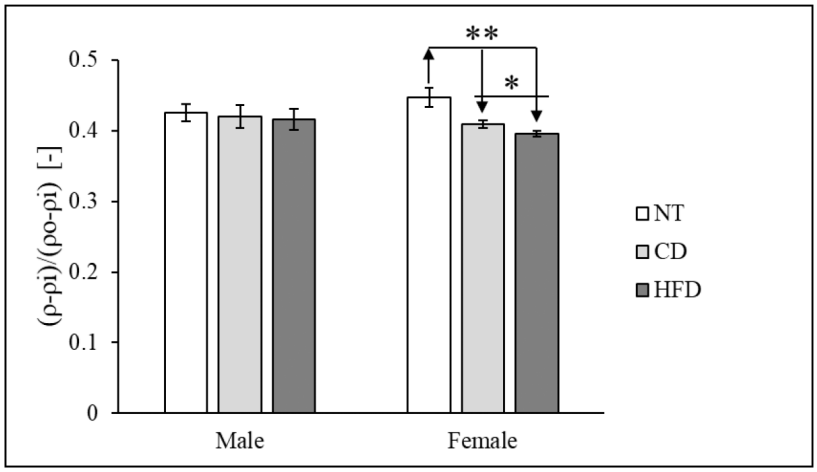

Figure 8.

Non-dimensional radial location of the circumferential neutral axis in intact tissue for all for all samples (mean ± standard error). Comparison between CD and HFD (also included data for NT).

Table 1.

Best-fit material parameters values estimated for the model presented in Equation (1) for each group, shown in terms of mean ± st.dev. Specifically, terms with the subscript “c” describe the isolated collagen fibers, terms with the subscript “m” describe the isolated myocytes. In full, the experimental groups in this section were (a) isolated collagen from Sprague Dawley rats (n=3 male, n=2 female) and Dahl-SS rats (males, n=2 HFD and n=2 CD; females n=2 HFD and n=2 CD), and (b) isolated myocytes from Sprague Dawley rats (n=3 male, n=3 female), and Dahl-SS rats (male, n=2 HFD and n=2 CD; female, n=2 HFD and n=2 CD). Note that from each animal, two rings were isolated and tested.

Group:	**c_c (kPa)**	**k_c [-]**	**c_m (kPa)**	**k_c [-]**
SD male	0.465 ± 0.225	31.09 ± 4.09	0.051 ± 0.031	36.26 ± 13.73
SD female	0.492 ± 0.312	32.83 ± 4.18	0.047 ± 0.011	38.67 ± 9.33
Dahl-SS male	0.091 ± 0.060	30.17 ± 5.55	0.054 ± 0.012	43.08 ± 19.90
Dahl-SS female	0.326 ± 0.325	32.75 ± 4.92	0.064 ± 0.016	31.23 ± 8.20